The paper was presented at the Eleventh Meeting
"New Trends in Fatigue and Fracture" (NT2F11)
Polignano a Mare, Italy, 3–6 July, 2011

Caterina Casavola, Carmine Pappalettere, Francesco Tattoli

FATIGUE BEHAVIOUR OF HYBRID Ti6Al4V CRUCIFORM WELDED JOINTS

ZAMOR HIBRIDNIH KRSTASTIH ZAVARENIH SPOJEVA Ti6Al4V

Originalni naučni rad / Original scientific paper
UDK /UDC: 621.791.05:669.295'71'292
669.295'71'292:539.431
Rad primljen / Paper received: 21.01.2012.

Adresa autora / Author's address:
Dipartimento di Ingegneria Meccanica e Gestionale,
Politecnico di Bari, Italy, email: casavola@poliba.it

Keywords
- fatigue
- titanium
- local method
- Wel.Fa.Re.
- cruciform joints

Ključne reči
- zamor
- titan
- lokalna metoda
- Wel.Fa.Re.
- krstasti spojevi

Abstract

This paper presents experimental fatigue results of titanium grade 5 (Ti6Al4V alloy) cruciform welded joints. The joining process used to realize the joints is the hybrid CO_2 laser-MIG welding technique. In this technique the laser beam is combined to the MIG arc in order to have advantages from both processes. The fatigue curves expressed in terms of nominal amplitude of stress (according to the traditional global method) and in terms of local amplitude of strain (according to the local Wel.Fa.Re. method) have been plotted after the experimental tests. Electrical strain gauges bonded close to the weld toe have been used to calculate the local strain amplitude. The fatigue tests have been carried out applying an axial loading to the specimen with a load ratio of 0.1. Finally a comparison with the fatigue resistance of hybrid butt welded joints is presented.

Izvod

U ovom radu su predstavljeni eksperimentalni rezultati ispitivanja zamora krstastih zavarenih spojeva od legure titana (gade 5 - Ti6Al4V). Postupak spajanja kojim je izvedeno formiranje spojeva je hibridni CO_2 laser-MIG postupak zavarivanja. Kod ovog postupka se kombinuje laserski snop sa MIG elektrolučnim postupkom zavarivanja radi postizanja prednosti oba postupka. Na osnovu eksperimentalnih ispitivanja, dobijene su krive zamaranja izražene preko nominalne amplitude napona (prema tradicionalnom globalnom postupku) i preko lokalne amplitude deformacije (prema lokalnom Wel.Fa.Re postupku). Upotrebljene su merne trake, postavljene blizu ivice šava, za izračunavanje amplitude lokalnih deformacija. Ispitivanja na zamor su izvedena primenom aksijalnog opterećenja sa odnosom 0.1. Konačno, predstavljeno je poređenje otpornosti na zamor hibridnih sučeono zavarenih spojeva.

INTRODUCTION

Titanium and its alloys are widely applied because of their favourable strength to weight ratio and their resistance to corrosion in oxidizing environments /1, 2/. The high corrosion resistance of titanium results from passivation by a thin oxide layer covering the surface. Obviously the oxide layer can only protect the metal as long as it remains intact.

High performance and concurrent weight become more and more important in the transport industry. In order to meet these demands, besides choosing lighter materials, welding is progressively replacing riveted structures. However, welding of titanium is not a simple process. It requires special care because titanium alloys have a high reactivity, especially at elevated temperature, with atmospheric gases. Furthermore, impurities could be absorbed in the welding pool. These drawbacks cause porosities and contamination resulting in a decrease of the mechanical resistance. Generally, the welding pool is protected by shielding gases using special devices. Helium and Argon are the most common inert gases used to protect the weld zone by oxidation and atmospheric contamination. Surface impurities have to be removed by chemical etching in order to avoid embrittlement of the weld zone.

Titanium alloys can be welded by several welding techniques and the most recent are laser beam welding (LBW) and laser-MIG hybrid welding (LAMIG) methods. In the laser beam welding process a high energy beam is focused on a narrow area. This results in a smaller heat affected zone compared with other welding techniques and in a high quality smooth weld cord. Porosities and smooth surface of the weld depend on process parameters. However the welding process can be studied and optimal parameters can be obtained in order to realize good quality welded joints. Compared with the LBW, the LAMIG welding technique can produce joints with higher ductility, due to the improvement of seam formation and lower microhardness, /3/. However, it is possible to carry out joints with no defects such as surface oxidation, porosity, cracks and lack of penetration in the welding seam with both methods, using the optimal parameters.

Design of welded joints is rather complicated because the weld toe can be considered as a geometrical discontinuity that modifies the stress distribution. Stresses near the weld toe are higher than the nominal stress and can even exceed locally the yield limit. Interactions between different factors (i.e. local and global geometry of the weld seam, microstructural modifications induced by material heating and cooling, residual stresses, etc.) affect the fatigue limit of welded structures by producing stress concentration near the weld toe.

Ti6Al4V is an α-β alloy (Titanium Grade 5 according to ASTM standards) with aluminium as an α-stabilizing, and vanadium a β-stabilizing element. It has a good weldability with both laser beam and hybrid laser-MIG welding techniques. The fatigue resistance of cruciform welded joints with no load carrying welds in Ti6Al4V obtained by hybrid (CO_2 laser and MIG) welding technique is studied in the present work. Fatigue strength curves in terms of both local strain amplitude, according to wel.fa.re. method /4-10/ and nominal stress amplitude are reported in the paper.

MATERIAL AND METHODS

Titanium grade 5 (Ti6Al4V) is an α-β alloy with aluminium that is an α-stabilizing element and vanadium that is a β-stabilizing element. This alloy has good mechanical properties at room and at high temperature. Its density is 4.4 kg/dm^3, /2/, the tensile strength is about 980 MPa and the yield strength is 760 MPa, /11/. The principal mechanical properties are reported in Table 1.

At room temperature, unalloyed titanium has a hexagonal close-packed (hcp) crystal structure called α-phase. At 883°C this transforms to a body centered cubic (bcc) structure called β-phase. The manipulation of these crystallographic variations through alloying additions and thermo-mechanical processing is the basis for the development of a wide range of alloys and properties. According to the standards, titanium grade 5 can contain other elements as reported in Table 2.

Table 1. Mechanical properties of grade 5 titanium alloy, /11/.
Tabela 1. Mehaničke osobine legure titana, /11/

Yield strength (MPa)	Ultimate strength (MPa)	Young's modulus (MPa)	Elongation at fract. (%)
760	980	110200	14

Table 2. Chemical composition of titanium grade 5 according to ASTM B265.
Tabela 2. Hemijski sastav legure titana prema ASTM B265

Element	C	Al	V	Fe	H	N	O
wt. %	<0.08	5.5-6.75	3.5-4.5	<0.30	<0.015	<0.03	<0.25

Impurities have important effects on transformation temperatures, lattice parameters and mechanical properties of titanium. Residual elements such as carbon, nitrogen, silicon and iron raise the strength and lower the ductility of titanium products. Basically, oxygen and iron contents determine strength levels of commercially pure titanium. In higher grades, oxygen and iron are intentionally added to the residual amounts already in the material to provide extra strength. On the other hand, carbon and nitrogen usually are held to minimal residual levels to avoid embrittlement. Aluminium is a principal alpha stabilizer in titanium alloys that increases tensile strength, creep strength and the elastic modules, /1/.

The joining process used to realize the cruciform joints is the hybrid CO_2 laser-MIG (LAMIG) welding. In this technique the laser beam is combined to the MIG arc in order to have advantages from both processes. The laser beam allows to have deeper welds, whereas the arc energy increases the welding speed. The laser power requirement in LAMIG method is lower compared to the LBW and it is possible to have smoother thermal cycles. Disadvantages of the laser welding technique are the insufficient gap bridging ability and the required precision in positioning. These drawbacks can be overcome by using the hybrid method, while maintaining the key advantages of laser welding and even improving the welding speed and penetration.

Compared with laser welded joints, hybrid welded joints have a better combination of strength and ductility, /3, 12/, and present less distortions. This is achieved by the high density energy producing a small pool and by the high travel speed.

Four plates of titanium grade 5 of the size 350 × 334 × 3 mm have been used in the study. The surfaces have been chemically cleaned before welding in order to eliminate surface contamination. The flanges are the size of 334 × 50 × 3 mm. Figure 1 shows the plate dimensions and the position of the welds.

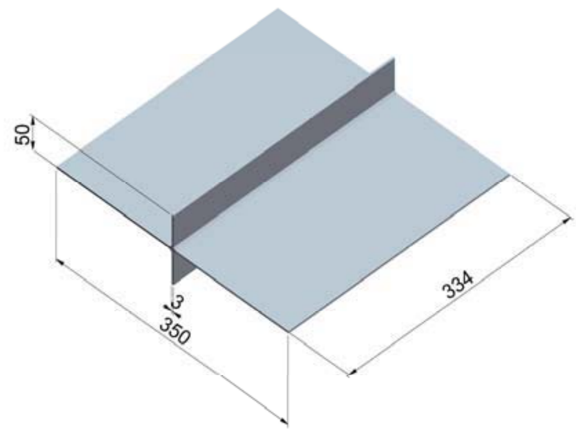

Figure 1. Ti6Al4V welded plate, dimensions of plates and flanges.
Slika 1. Zavarena ploča Ti6Al4V, dimenzije ploče i prirubnica

Table 3 shows the LAMIG welding parameters. A filler metal of similar chemical composition to the parent metal is used. During welding operations, all plates are constrained in 3 points in order to avoid the opening of the junction. The weld traces are subsequently cross out by the following welding passage.

Table 3. Summary of the laser-MIG welding parameters.
Tabela 3. Parametri laser-MIG postupka zavarivanja

Laser CO_2 power (W)	2300
MIG Power (W)	9000
Distance laser-MIG (mm)	0
Welding velocity (m/min)	2
Wire velocity (m/min)	5
Gas for plasma suppression	He
Shielding gas	Ar

Rectangular fatigue specimens are machined from the welded plates with their welded flanges located in the middle of the length. The width of each specimen is about 50 mm. Outer sides of plates are removed because of defects and welding irregularities (often the cord has a golden colouration in these zones as a consequence of partial oxidation caused by some problems in protecting the initial and final part of the plate).

Fatigue tests are carried out on a servo-hydraulic machine (SCHENCK 250 kN) and on a mechanical resonance machine (RUMUL Vibro-forte 500 kN) under constant amplitude loading and a load ratio R = 0.10. The frequency of the load is set to 15 Hz for the test carried out on the servo-hydraulic machine. In the mechanical resonance machine the frequency depends on the specimen geometry and material. In this work the frequency is about 60 Hz.

Before the execution of the tests, two strain gauges have been bonded on each side of the specimen in order to measure the local strain amplitude. Figure 2 shows the disposition of the strain gauges on the specimen.

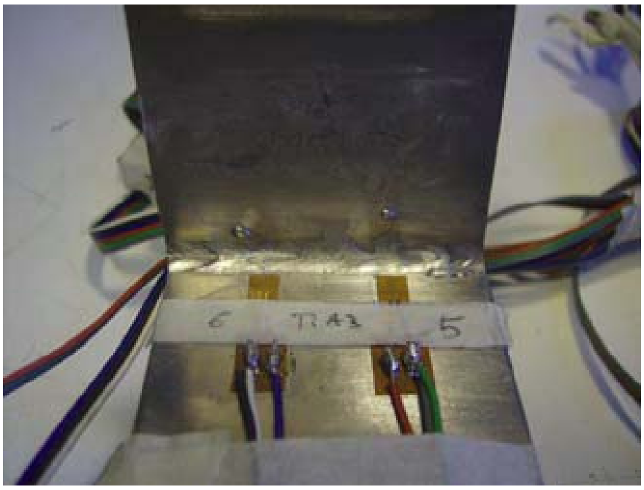

Figure 2. Disposition of strain gauges on the welded specimen.
Slika 2. Položaj mernih traka na zavarenom uzorku

The strain gauges used in this work have 3 mm grid length. They are bonded with their transversal axis at 2.5 mm from the cord. The grid is placed between 1 and 4 mm from the weld toe. The position of strain gauges and the grid dimension results from a compromise between the two requirements: the need to correctly evaluate the local strain field in the critical zone, which requires measurements in the region very close to the weld toe and the use of a reliable and friendly experimental technique which may be transferred to an industrial environment, /7, 13/. Strain gauge grid location adopted in the Wel.Fa.Re. method is chosen with the purpose to capture local effects as the joint global geometry, misalignments, welding local geometry, and plasticity, that are relevant for the fatigue phenomena and which influence the strain field at the weld toe.

The Wel.Fa.Re. method utilises the local strain amplitude ε_a measured at the weld toe, /9/, because it presumes that this parameter can include the effects of all variable influencing the fatigue life of welded joints. The local strain amplitude is measured before the fatigue test by applying a static nominal load amplitude. Consequently, with the execution of the fatigue tests it is possible to obtain the fatigue life curve expressed in terms of local strain amplitude ε_a:

$$\varepsilon_a = \frac{\varepsilon_{\max} - \varepsilon_{\min}}{2}$$

and in terms of nominal stress amplitude σ_a:

$$\sigma_a = \frac{\sigma_{\max} - \sigma_{\min}}{2}$$

Before fatigue tests, a visual inspection is executed on all specimens in order to examine the quality of the cord. The cord has a silver colouration which indicates good gas protection without contamination and oxidation. Eight electrical strain gauges are bonded on the specimens according to Wel.Fa.Re. guidelines. Local strain is measured at the weld toe. Strain gauge measured values are registered by System 5000, by Micro Measurements Inc. (USA).

TEST PLAN

Four Ti6Al4V hybrid welded plates are used in this work and six specimens are cut from each plate. Before the execution of the tests, the α angle (Fig. 3) is measured in order to evaluate the secondary bending effect on fatigue tests. The distortion of the plates is caused by the welding thermal cycle. The heating and subsequent cooling of a narrow area and the gradient of temperature imposed to the plate are the causes of distortions and residual stresses in the welded joints.

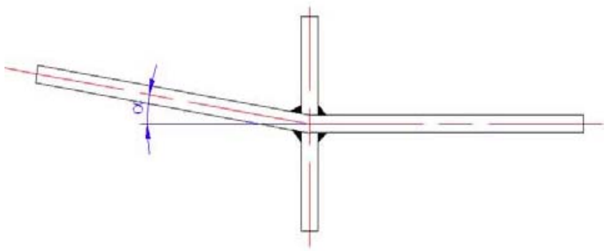

Figure 3. Distortion angle on the specimen after the weld process.
Slika 3. Ugao distorzije uzorka posle zavarivanja

Table 4 reports the values of the distortion angle α measured on the specimens, obtained from the four welded plates. The α angle has a very low value with a mean value of 0.4°. In the nomenclature of the specimens, the letter refers to the plate and the number to the specimen number.

A careful observation of the joints leads to affirm that there is a slight misalignment of the flanges, as shown in Fig. 4, for few joints.

The value of this misalignment is variable, however its maximum is about 2 mm.

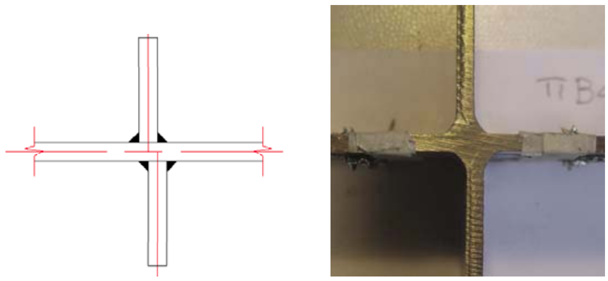

Figure 4. Some welded joints present flange misalignment.
Slika 4. Neki zavareni spojevi imaju smaknutost prirubnice

Table 4. Distortion angle α measured on the test specimens.
Tabela 4. Ugao distorzije α izmeren na uzorcima

Specimen	Distortion angle α (°)
A1	0.38
A2	0.32
A3	0.17
A4	0.37
A5	0.53
A6	0.80
mean value	0.43
standard deviation	0.22
B1	0.66
B2	0.64
B3	0.50
B4	0.55
B5	0.52
B6	0.19
mean value	0.51
standard deviation	0.17
C1	0.37
C2	0.21
C3	0.29
C4	0.47
C5	0.47
C6	0.37
mean value	0.36
standard deviation	0.10
D1	0.35
D2	0.42
D3	0.34
D4	0.38
D5	0.44
D6	0.20
mean value	0.36
standard deviation	0.08

RESULTS AND DISCUSSION

All fatigue tests are performed with a load ratio R = 0.1. The frequency depends on the testing machine used. Fatigue test results are summarized in Table 5. The table reports the values of the nominal stress amplitude σ_a, the local strain amplitude ε_a, the number of cycles to failure N, and the final crack location.

Specimens obtained from A and B plates are tested on the Schenck servo-hydraulic machine. The frequency of the fatigue load is 15 Hz. Specimens from C and D plates, instead, are tested on the Rumul resonance machine. The frequency of the fatigue load for these specimens is in the range 64-68 Hz. The loading frequency does not influence fatigue resistance significantly when the applied stress range is low and the frequency is less than 50 Hz, /14/. When the stress range is high, capable of producing plastic deformation with each cycle of loading (low cycle of fatigue) an increase in the frequency produces an increase in the apparent fatigue strength.

The final fracture is generally located at the weld toe. Only for few specimens the fatigue final fracture is within the nominal zone (Fig. 5).

Fatigue curves in terms of nominal amplitude of stress σ_a-N and local amplitude of strain ε_a-N are reported in Figs. 6 and 7.

Table 5. Experimental results.
Tabela 5. Eksperimentalni rezultati

Specimen	Nominal stress amplitude σ_a (N/mm^2)	Local strain amplitude ε_a (με)	Cycles to failure N	Final crack location
A1	70.70	691.5	376723	weld toe
A2	66.96	678.0	734103	weld toe
A3	62.55	627.2	10200382	unbroken
A4	78.11	749.9	332215	weld toe
A5	82.82	776.3	379238	weld toe
A6	74.10	717.0	396165	weld toe
B1	93.89	887.1	238227	weld toe
B2	52.23	509.2	6232722	unbroken
B3	52.14	486.9	11000000	unbroken
B4	71.56	670.7	1878897	nominal zone
B5	80.42	752.2	395298	weld toe
B6	75.53	743.4	491531	HAZ
C1	50.13	586.0	479348	weld toe
C2	43.60	549.5	1200000	nominal zone
C3	50.34	584.5	736834	weld toe
C4	49.26	589.0	475218	weld toe
C5	48.16	559.0	10139780	unbroken
C6	49.86	566.5	1388372	nominal zone
D1	62.74	711.8	246987	weld toe
D2	59.79	747.0	214651	weld toe
D3	50.09	709.0	231181	weld toe
D4	36.29	464.0	10852620	unbroken
D5	47.98	554.0	977257	weld toe
D6	52.99	552.8	4487500	weld toe

(a)

(b)

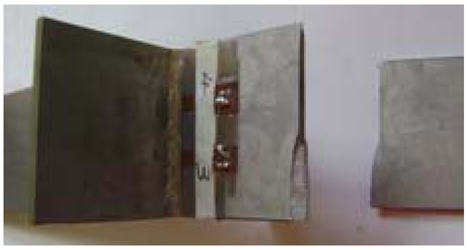

(c)

Figure 5. Three different fatigue fracture locations for the cruciform no-load carrying Ti6Al4V hybrid welded joints: (a) at the weld toe; (b) within the nominal zone; (c) within the HAZ.
Slika 5. Tri različita mesta loma usled zamora za krstaste neopterećene hibridne zavarene spojeve Ti6Al4V: (a) na ivici šava; (b) unutar nominalne zone; (c) unutar ZUT

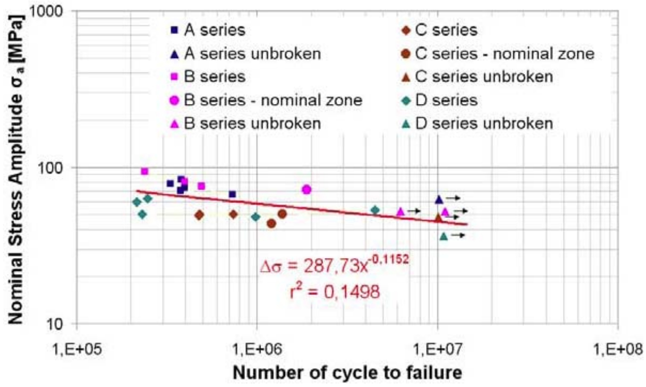

Figure 6. Fatigue curve σ_a-N.
Slika 6. Kriva zamaranja σ_a-N

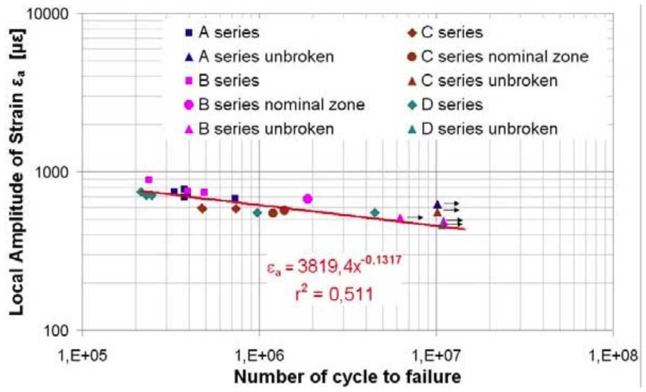

Figure 7. Fatigue curve ε_a-N.
Slika 7. Kriva zamaranja ε_a-N

Figures 6 and 7 show that C and D plates have a lower fatigue strength, but this is due to weld imperfections and irregularities as shown in Fig. 8. It should be noted, in fact, that the fatigue curve expressed in terms of local amplitude of strain has a higher correlation factor, and points obtained from C and D specimens are very close to the A and B specimens. However, the fatigue trend of C and D specimens is a little lower than the A and B trend and it could be due to the different loading frequency.

(a)
(b)

Figure 8. Weld cords: a) A and B plates; b) C and D plates.
Slika 8. Konture zavara: a) ploče A i B; b) ploče C i D

Generally, in many industrial applications, the nominal stress approach is prevailing compared to the local method concept in the design of welded structures. The application of the nominal stress concept requires two important definitions: definition of nominal stress and its permissible value with reference to a corresponding classified structural detail. In design codes /15-19/, the fatigue design categories of welded structures detail are called FAT which means fatigue design class. The number following this abbreviation is the allowable nominal stress range $\Delta\sigma$ expressed in MPa at $N = 2 \times 10^6$ cycles. The fatigue life number of cycles, instead, consists of the crack initiation life and the subsequent long-crack propagation life up to final fracture. In unnotched specimens the microstructural crack initiation could be prevalent in the total fatigue life, while in sharply notched specimens, the crack initiation life may be very short. However, in the case of more complex structural details, to which neither a nominal stress nor a design category can be assigned, only the local concept is applicable /4-10, 20/. The fatigue process has a local character and cannot be well described by global (nominal) stress and this justifies the test results. All welded specimens belong to the same classified structural detail according to the global approach, but they have different fatigue strengths, in terms of stress amplitude, due to the different weld cord profile. Local approaches, such as the Wel.Fa.Re. method, instead can account for the effects of all local factors influencing fatigue life of welded joints. For this reason, local methods can provide useful indications also in cases where there are no specific standards. Strain gauge grid position used in Wel.Fa.Re. is useful for capturing local effects due to joint global geometry, misalignments, local geometry, plasticity, that are relevant for the fatigue phenomena and can affect the strain field at the weld toe.

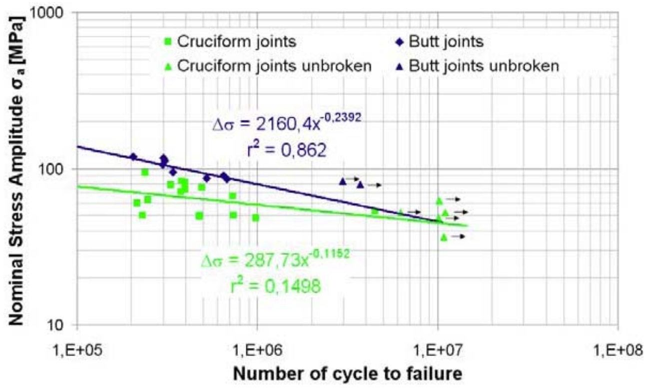

Figure 9. σ_a-N fatigue curves of cruciform and butt joints.
Slika 9. σ_a-N krive zamaranja za krstaste i sučeone spojeve

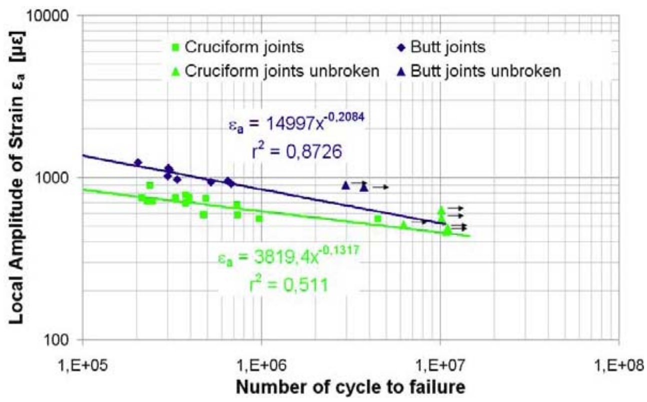

Figure 10. ε_a-N fatigue curves between cruciform and butt joints.
Slika 10. ε_a-N krive zamaranja za krstaste i sučeone spojeve

The fatigue strength of titanium grade 5 cruciform joints with no load carrying fillet weld is obviously less than static strength and fatigue strength of hybrid butt welded joints. In Figs. 9 and 10, the fatigue curves for cruciform welded joints and butt welded joints obtained by the hybrid welding technique in terms of nominal stress amplitude and local strain amplitude are compared.

Experimental data are summarized in Table 6. Fatigue strength reference values σ_a are calculated at 2 million, 5 million and 10 million cycles from experimental results.

Table 6. Summary of experimental results.
Tabela 6. Pregled eksperimentalnih rezultata

Type of joint	Fatigue strength N=2·10^6 (MPa)	Fatigue strength N=5·10^6 (MPa)	Fatigue strength N=10·10^6 (MPa)
butt	67	54	46
cruciform	54	49	45

CONCLUSION

The fatigue behaviour of cruciform hybrid welded joints in titanium grade 5 is studied. σ_a-N and ε_a-N fatigue curves are obtained. The ε_a-N fatigue curve is plotted according to Wel.Fa.Re. method recommendations: two electric strain gauges are bonded with their principal axes at 2.5 mm from the weld toe for each weld cord, then the local strain amplitude is calculated by applying the maximum and minimum load in the fatigue test. The Wel.Fa.Re. method is a local approach in fatigue design. It presumes that the local strain amplitude is an important variable in describing the fatigue behaviour of welded joints independently from the shape and for this reason it can provide useful indications also in cases where there are no specific standards.

The local strain amplitude can account for the effects of many factors influencing fatigue life of welded joints and that the nominal stress concept could not appreciate. In fact, for Ti6Al4V cruciform joints, the fatigue curve expressed in terms of local strain amplitude ε_a has a higher correlation factor than the classical σ_a-N curve. The local strain amplitude can estimate the differences in the weld cord geometry and its effect on the local stress-strain field. The Wel.Fa.Re. method, however, can appreciate all other factors influencing the fatigue behaviour, such as joint global geometry, misalignments, plasticity, except for residual stresses.

Finally, a comparison with the fatigue resistance of the Ti6Al4V butt hybrid welded joints is presented. Cruciform joints have a lower fatigue resistance, but the difference is higher at a low number of cycles to failure. In fact, the two fatigue curves have a different slope.

REFERENCES

1. ASM International. ASM Handbook Properties and Selection: Nonferrous Alloys and Special - Purpose Materials, Vol.2, 1992.
2. ASTM B265, Standard Specification for Titanium and Titanium Alloy Strip, Sheet and Plate. 2006.
3. Li, R., Li, Z., Zhu, Y., Rong, L., *A comparative study of laser beam welding and laser-MIG hybrid welding of Ti-Al-Zr-Fe titanium alloy*, Materials Science and Engineering A, 528: 1138-1142, 2011.
4. Casavola, C., Nobile, R., Pappalettere, C., *Fatigue strength by the wel.fa.re. local strain method: application to 3-5 mm cruciform and butt welded joints*, SEM Annual Conference and Exposition on Experimental and Applied Mechanics, Milwaukee (USA), 2002.
5. Casavola, C., Nobile, R., Pappalettere, C., *Fatigue life predictions by the wel.fa.re. method: influence of residual stresses*, SEM Annual Conference and Exposition on Experimental and Applied Mechanics, Charlotte (USA),.2003.
6. Casavola, C., Nobile, R., Pappalettere, C., *A local strain method for the evaluation of welded joints fatigue resistance: the case of thin main – plates thickness*, Fatigue & Fracture of Engineering Materials & Structures, 28:759-767, 2005.
7. Casavola, C., Pappalettere, C., *Industrial application of a new local strain method for fatigue strength evaluation of welded structures*, ICEM 12 International Conference on Experimental Mechanics, Bari (Italy), 2004.
8. Casavola, C., Pappalettere, C., *Application of wel.fa.re. method on aluminium alloy welded joints*, SEM Annual Conference and Exposition on Experimental and Applied Mechanics, Portland (USA), 2005.
9. Dattoma, V., Nobile, R., Panella, F.W., *Some considerations on the local strain amplitude used in the wel.fa.re. method as a design parameter against fatigue*, Proceedings of the International Conference New Trends in Fatigue and Fracture II, Hammamet (Tunisia), 2003.
10. Pappalettere, C., Nobile, R., *Fatigue strength of welded joints by the local strain method. Influence of load ratio R and plate thickness, notch effects in fatigue and fracture*, Pluvinage G., Gjonanj M. (Eds.), NATO Sciences Series II – Mathematics, Physics and Chemistry, Kluwer, 307-316, 2000.
11. Casavola, C., Pappalettere, C., Tattoli, F., *Experimental and numerical study of static and fatigue properties of titanium alloy welded joints*, Mechanics of Materials, 41:231-243, 2009.
12. Li, C., Muneharua, K., Takao, S., Kouji, H., *Fiber laser-GMA hybrid welding of commercially pure titanium*, Materials and Design, 30:109-114, 2009.
13. Haibach, E., Die Schwingfestigkeit von Schweibverbindungen aus der Sicht einer örtlichen Beanspruchungsmessung, LBF – Bericht no. FB-77, Lab. f. Betriebsfestigkeit, Darmstadt, 1968.
14. Masubuchi, K., Analysis of Welded Structures, Pergamon Press, Oxford, NY, 1980.
15. Eurocode 3. Design of steel structures. Part 1-9: Fatigue, UNI ENV 1993-1-9. European Committee for Standardization, 2005.
16. Eurocode 9. Design of aluminium structures. Part 2: structures susceptible to fatigue, UNI ENV 1999-2. European Committee for Standardization, 2002.
17. BS 7608. Fatigue design and assessment of steel structures. London: British Standards Institute, 1993.
18. Recommendations of IIW. XIII-1593-96/XV-845-96. Fatigue design of welded joints and components, Abington Publishing, Cambridge, 1996.
19. AWS D 1.9/D 1.9/M. Structural Welding Code – Titanium, 2007.
20. Radaj, D., Sonsino, C.M., Fatigue Assessment of Welded Joints by Local Approaches, Abington Publishing, Cambridge, 1998.